

## Reflection image beyond the known extent of the prospective zone provided by 3D virtual-source methodology

Chamarczuk, M.; Draganov, D.; Malinowski, M.; Koivisto, E.; Heinonen, S.; Rötsä, S.

**DOI**

[10.3997/2214-4609.202210151](https://doi.org/10.3997/2214-4609.202210151)

**Publication date**

2022

**Document Version**

Final published version

**Published in**

83rd EAGE Conference and Exhibition 2022

**Citation (APA)**

Chamarczuk, M., Draganov, D., Malinowski, M., Koivisto, E., Heinonen, S., & Rötsä, S. (2022). Reflection image beyond the known extent of the prospective zone provided by 3D virtual-source methodology. In *83rd EAGE Conference and Exhibition 2022* (pp. 572-576). EAGE. <https://doi.org/10.3997/2214-4609.202210151>

**Important note**

To cite this publication, please use the final published version (if applicable). Please check the document version above.

**Copyright**

Other than for strictly personal use, it is not permitted to download, forward or distribute the text or part of it, without the consent of the author(s) and/or copyright holder(s), unless the work is under an open content license such as Creative Commons.

**Takedown policy**

Please contact us and provide details if you believe this document breaches copyrights. We will remove access to the work immediately and investigate your claim.

***Green Open Access added to TU Delft Institutional Repository***

***'You share, we take care!' - Taverne project***

**<https://www.openaccess.nl/en/you-share-we-take-care>**

Otherwise as indicated in the copyright section: the publisher is the copyright holder of this work and the author uses the Dutch legislation to make this work public.

## REFLECTION IMAGE BEYOND THE KNOWN EXTENT OF THE PROSPECTIVE ZONE PROVIDED BY 3D VIRTUAL-SOURCE METHODOLOGY

M. Chamarczuk<sup>1</sup>, D. Draganov<sup>2</sup>, M. Malinowski<sup>3</sup>, E. Koivisto<sup>4</sup>, S. Heinonen<sup>3</sup>, S. Röttsä<sup>5</sup>

<sup>1</sup> Institute of Geophysics PAS; <sup>2</sup> Delft University of Technology; <sup>3</sup> Geological Survey of Finland; <sup>4</sup> University of Helsinki; <sup>5</sup> Boliden Kevitsa Mining Oy

### Summary

---

We apply a full-scale 3D seismic virtual-source survey (VSS) for the purpose of near-mine mineral exploration in the Kylylahti sulfide deposit, Finland. Based on the ambient-noise (AN) characterization including beamforming results, we created a 10-days subset of AN recordings that were dominated by multi-azimuth high-velocity arrivals. We use an illumination-diagnosis and location procedure to show that the AN recordings associated with the high apparent velocities are related to body-wave events. Next, we produce 994 virtual-source gathers by applying seismic-interferometry processing by cross-correlating AN at all receivers resulting in a full 3D VSS. We apply standard 3D time-domain reflection-data processing and imaging using the subset and the full AN data, and validate both results against a pre-existing detailed geological information and 3D active-source data processed in the same way as the passive data. The resulting post-stack migrated sections show agreement of reflections between the passive and active data and indicate that VSS provides images where the active-source data are not available. In particular, the previously unknown extent of the ore-bearing complex was captured exclusively by passive data, which added a new geological insight into the Kylylahti formation. The methodological approach developed can be used in other areas in mineral exploration context.

## Reflection image beyond the known extent of the prospective zone provided by 3D virtual-source methodology

### Introduction

Our study elaborates on many pioneering works in ambient-noise seismic interferometry (ANSI) imaging experiments (Draganov et al. 2013, Cheraghi et al. 2015, Nakata et al. 2015, Olivier et al. 2015), by investigating the potential of the full-scale 3D virtual seismic survey (VSS) to image sub-vertical, complicated geological target, and potentially indicate the continuity of ore resources in the mine-infrastructure vicinity. The final outcome of the 2D ANSI reconnaissance study in the Kylylahti area in Finland (Chamarczuk et al. 2021) provided the initial delineation of the ore-bearing formation, which justified our decision to conduct the follow-up 3D investigation with the seismic-interferometry processing workflow indicated by the initial 2D ANSI assessment. Here, we report the results of this first hardrock full-scale 3D passive experiment, and put the special emphasis on describing the geological insights obtained using the 3D VSS methodology.

### Apriori geological knowledge

Because of the complex geometry (see cross-section in Figure 1), the Kylylahti formation remains a difficult target for surface seismic methods. Nevertheless, the end-goal of proposing the 3D VSS methodology (Figure 2), developed as a part of Kylylahti experiment, is the conventional reflection processing of the virtual-source gathers (VSGs) and their comparison with the active-source processing results as well as with the available detailed geological data and models. We focus on describing the geological insights provided by our passive experiment. Our apriori geological knowledge in the Kylylahti area, based on Peltonen et al. (2008), can be summarized as follows: in the Kylylahti area, four main geological units are present (Figure 1) – (1) The Kylylahti semi-massive to massive sulfide (S/MS) mineralization hosted in (2) Outokumpu ultramafics (OUM) that mainly consist of serpentinite and talc-carbonate rocks with (3) fringed alteration zones composed of carbonate-skarn-quartz rocks, the altered Outokumpu ultramafics (OME). In combination, the nearly N-S trending and near-vertical OUM and OME units are called the Outokumpu assemblage rocks (referred to as Kylylahti formation). In the Kylylahti area, the Outokumpu assemblage rocks are in near-vertical contact with the (4) regional Kaleva Sedimentary Belt (KAL), consisting of mica schist and black schist. Besides the obvious strong impedance contrast between the S/MS mineralizations and the host rocks, rock-property measurements (Luhta et al. 2016) indicate sufficiently strong contrasts in acoustic impedances, in the Kylylahti area mainly arising from contrasts in densities, to produce a detectable reflection at the contact of the OUM/OME rocks and the inter-layered and surrounding schists.

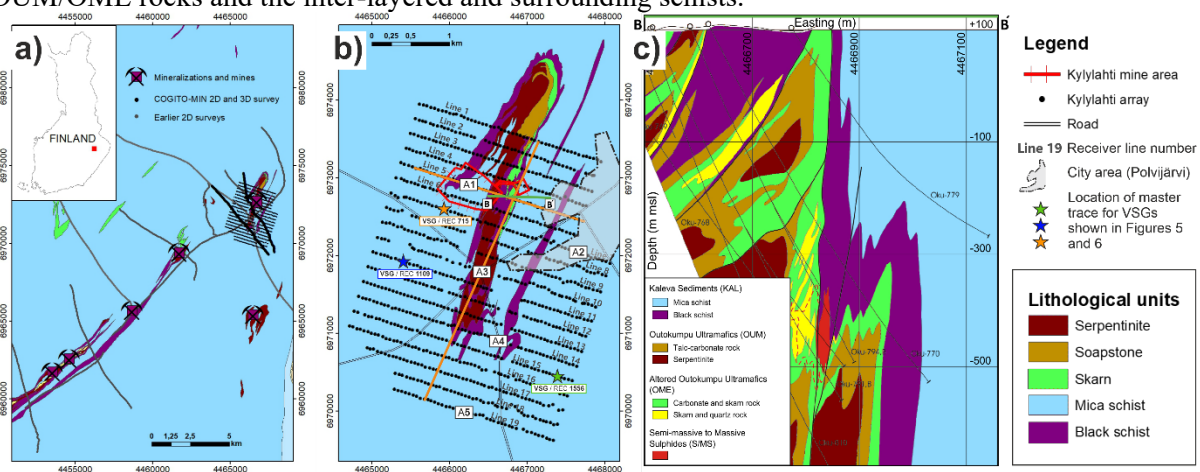


**Figure 1** (a) Location of the Kylylahti mine and Kylylahti array in the Outokumpu belt. (b) Location of the 3D passive seismic survey. (c) B-B' is a cross-section through the Kylylahti deposit (modified after Peltonen et al. (2008) and Riedel et al. (2018)).

### 3D VSS Reflection imaging methodology

The 3D VSS methodology adopted in this study can be summarized as follows: (1) general analysis of the recorded wavefield to identify dominant frequencies, directions of illumination and apparent velocities of the AN wavefields; (2) quantification of body-wave energy present in the recorded data using the TWEED approach (see Chamarczuk et al. 2021 for more details) and obtaining spatial distribution of the noise sources; (3) actual SI data retrieval, i.e., obtaining VSGs through cross-correlation for the two sets of data – (i) for 10 days when body-wave events are dominating and (ii) for the full 30 days of data; (4) standard hardrock reflection seismic processing of the obtained VSGs. The above 4 processing steps together with validation and interpretation of passive results using a direct comparison to an active survey as a benchmark, and to the available detailed geological data and models as a reference, add up to the 5 main processing blocks forming the full-scale 3D seismic VSS methodology for the purpose of near-mine mineral exploration developed in this study (see flowchart in Figure 2, where the gray-gradient-colored blocks in the right column indicate our modifications of the state-of-the-art AN imaging workflow proposed by Draganov et al., 2013).

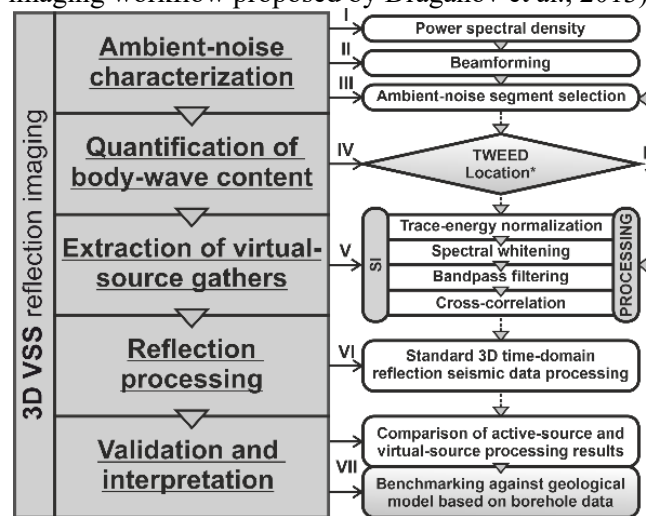


**Figure 2** Summary of the 3D virtual-source survey methodology for the purpose of near-mine mineral exploration. The left column presents the core of the flowchart containing five main processing blocks. The detailed processing steps performed within each main processing block are shown in the right column. The sequence of processing is indicated by roman numerals. Gray-gradient-colored blocks in the right column indicate our modifications of the state-of-the-art ambient-noise imaging workflow proposed by Draganov et al. (2013).

### Selected processing results

In Figure 3a, we show the results of standard beamforming analyses (e.g., Nakata et al. 2015) calculated and summed over 20 hours recorded during each single day in the frequency range between 3 to 5 Hz. These daily beamforming plots represent the dominant AN contributions during each single day of the Kylylahti passive acquisition (30 days). We used these results to identify periods of data associated predominantly with P-wave arrivals, and to create a subset of 10 days used for further processing (green circles in Figure 3a). Next, we used dedicated detection and location procedure to verify that the high-velocity arrivals observed in the beamforming (green circles in Figure 3a) are actually related to body-wave events and not to some crossline surface-wave sources. Figure 3b shows an example of a noise panel containing a clear body-wave event representative for day 3 (‘D3’ in Figure 3a). We used daily recordings having body-wave content to create the input subset for the SI processing routine denoted as processing block ‘V’ in Figure 2. As a results of the SI processing, we obtained VSG that can be input for conventional active-source reflection imaging workflow. Figure 3c shows a comparison of the common source gathers obtained along 4 receiver lines, where arrows with the same colours on both active- and virtual-source gathers indicate reflection events associated with the same geological features.

## Geological features interpreted from the passive data

The availability of the coincident active-source 3D data provides an opportunity to compare the passive processing results directly with the active-source data. In Figure 4, we show comparison of the 3D processed images along crossline 1068, of the active survey (Figure 4a), and passive survey obtained using selectively stacked 10 days (Figure 4b,c) with the overlaid geological model based on borehole data. The predominant features visible in both active and passive data are a reflection related to the internal contacts within the Kylylahti formation hosting mineralization (see event marked with arrow 5 in Figure 4) and a dipping event (denoted with arrows 6-8), which corresponds to the base of the Kylylahti formation. Specifically, we highlight here the continuous and coherent reflection event correctly aligned with the OUM/OME part of the geological model, which starts at the position of arrow 6 in the active-source data (Figure 4a). The same event (following the general dipping trend of the orebody) is visible in the passive data. However, as indicated with arrows 7 and 8 (see Figure 4b,c), the exclusive added value of the passive data is the retrieval of the prolongation of the same event that extends beyond the known extent of the Kylylahti body (i.e., the bottom of the density model).

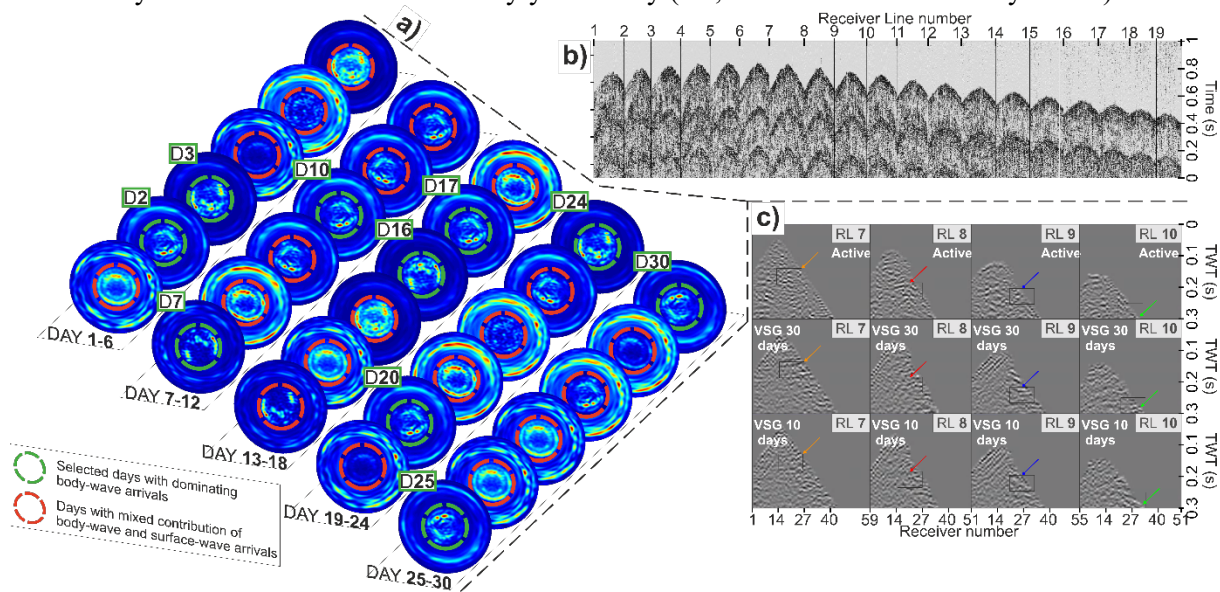


**Figure 3** (a) Directional beamforming analysis of recorded ambient noise (AN) calculated for 20 hourly panels from 30 days of recording time. (a) Panels representing analysis for one day of recording. Green dashed circles highlight ten daily AN recordings dominated by arrivals with apparent velocities  $>4.8$  km/s and used for initial selection of the 10-days subset as the representation of the selective-stacking approach in this study. (b) Scheduled mine event (underground blast) detected with TWEED, and representing the typical body-wave event recorded by the Kylylahti array. (c) Comparison of exemplary co-located 3D common-source gathers using active and passive data. For each gather, we show 4 receiver lines (RL). Common-source gathers co-located with receiver station 715: (top row) active-source gathers, (middle row) virtual-source gathers (VSGs) obtained using 30 days of noise, (bottom row) VSGs obtained using 10 days of noise.

## Conclusions

We investigated the imaging potential of large-N passive seismic arrays for near-mine exploration in conjunction with a developed methodology for body-wave reflections retrieval using seismic interferometry. By comparing the results of the passive seismic survey to active-source seismic data and pre-existing detailed geological models from the target area, this first hardrock full-scale 3D passive experiment confirmed the feasibility of virtual-source surveys to provide interpretable reflection image of structures beyond the known extent of the prospective zones. We also showed that passive survey can provide new insights not captured by the active-source seismic data or other earlier data sets. In particular, some of the reflective segments arising from critical lithological contacts (considering understanding the extent of the ore-bearing complex and the mineral exploration in the area) were



captured with the passive data better, and this allowed to add valuable new constraints for the detailed geological model built based on data sets available from the area.

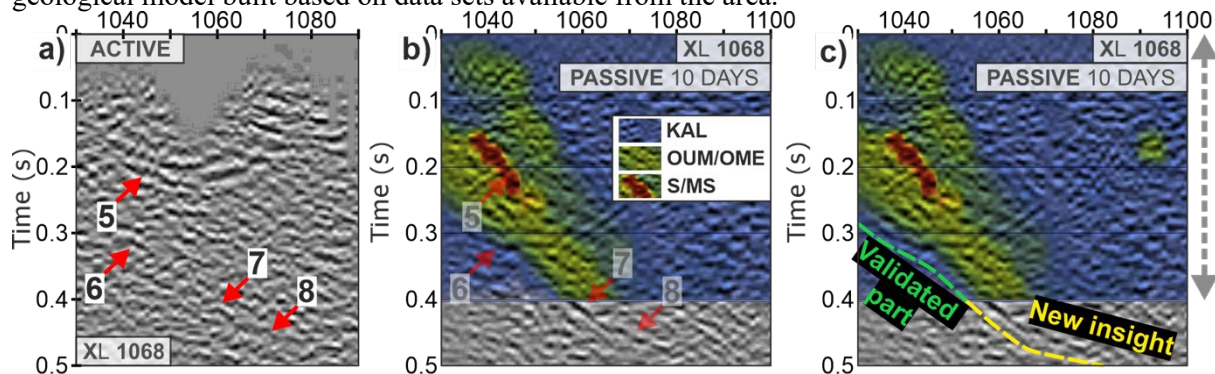


**Figure 4** Comparison of post-stack migrated sections obtained from the (a) active and (b, c) passive surveys. Red arrows mark the reflection events that are associated with the contacts in the geological model, and numbers show reflections that are interpreted in the text. The geological model displayed in the background is color-coded as follows: S/MS mineralisation (red); OUM/OME units (green); KAL unit (blue). Dashed line in (c) indicates the dipping reflection event corresponding to the base of the shown OUM/OME unit, where the green part is the part validated by the geological model based on borehole data, while the yellow part shows part of the same reflector that provided new geological insight by showing the previously unknown extent of the Kylylahti formation. Grey dashed line in (c) denotes the extent of the geological model before the Kylylahti passive experiment.

## References

- Chamarczuk, M., Malinowski, M. and Draganov, D. [2021] 2D body-wave seismic interferometry as a tool for reconnaissance studies and optimization of passive reflection seismic surveys in hardrock environments, *J. Appl. Geophys.*, 187, 104288, 2021.
- Cheraghi, S., Craven, J. A. and Bellefleur, G. [2015] Feasibility of virtual source reflection seismology using interferometry for mineral exploration: A test study in the Lalor Lake volcanogenic massive sulphide mining area, Manitoba, Canada. *Geophysical Prospecting*, 63(4), 833-848.
- Draganov, D., Campman, X., Thorbecke, J. W., Verdel, A. and Wapenaar, K. [2013] Seismic exploration-scale velocities and structure from ambient seismic noise (>1 Hz). *J. Geophys. Res. Solid Earth*, 118(8), 4345-4360.
- Luhta, T., Mertanen, S., Koivisto, E., Heinonen, S., Törmälehto, T. and Kukkonen, I. [2016] The seismic signature of the Kylylahti deposit: Initial results from new petrophysical measurements, *Lithosphere 2016, Programme and Extended Abstracts*, 79-82.
- Nakata, N., Chang, J. P., Lawrence, J. F. and Boue, P. [2015] Body wave extraction and tomography at Long Beach, California, with ambient-noise interferometry. *J. Geophys. Res. Solid Earth*, 120(2), 1159-1173.
- Olivier, G., Brenguier, F., Campillo M., Lynch R. and Roux, P. [2015] Body-wave reconstruction from ambient noise seismic noise correlations in an underground mine. *Geophysics*, 80(3), KS11-25.
- Peltonen, P., Kontinen, A., Huhma, H. and Kuronen, U. [2008] Outokumpu revisited: New mineral deposit model for the mantle peridotite-associated Cu–Co–Zn–Ni–Ag–Au sulphide deposits, *Ore Geol. Rev.*, 3(3), 559-617.
- Riedel, M., Cosma, C., Enescu, N., Koivisto, E., Komminaho, K., Vaitinen, K., and Malinowski, M. [2018] Underground Vertical Seismic Profiling with Conventional and Fiber-Optic Systems for Exploration in the Kylylahti Polymetallic Mine, Eastern Fin Land, *Minerals*, 8(11), 538.